Characterization Study of Dyes Photodegradation-Adsorption Products by TiO₂-Chitosan Immobilized on Glass Beads using Flow System

Bella Sukma Mahadika[1], Asep Saefumillah[1*], Saepurahman Saepurahman[2], Kiki Adi Kurnia[3], Diana Vanda Wellia[4]

[1]Department of Chemistry, Faculty of Mathematics and Natural Sciences, Universitas Indonesia
Jalan Lingkar Kampus Raya, Pondok Cina, Beji, Depok, 16424, Indonesia
[2]Center for Advanced Chemistry Research, National Research, and Innovation Agency (BRIN)
Jalan PUSPITEK Building 452, Muncul, Serpong, South Tangerang, 15314, Indonesia
[3]Department of Chemical Engineering, Faculty of Industrial Technology, Institut Teknologi Bandung
Labtek X Building No. 12, Jalan Ganesha, Lebak Siliwangi, Coblong, Bandung, 40132, Indonesia
[4]Department of Chemistry, Faculty of Mathematics and Natural Sciences, Universitas Andalas
Limau Manis, Pauh, Padang, 25163, Indonesia

*Corresponding author: asep.saefumillah@sci.ui.ac.id

Abstract

Dyes have a complex molecular structure that is difficult to degrade and can persist for a long time in water bodies. This study examines more thoroughly the effectiveness of photodegradation-adsorption of dyes, kinetic aspects, isotherms, thermodynamics, identification of the structure of photodegradation products, and changes in environmental quality parameter values whose results are quite satisfactory. The combination of photodegradation-adsorption of dyes by TiO₂-chitosan modified glass beads using a flow system has never been accomplished before. Flowing of the dye resulted in a dye degradation efficiency of 99%. The FESEM-EDX analysis shows that TiO₂-chitosan has been coated onto the surface of the glass beads. R^2 of kinetics MB, MO, RB are 0.99234, 0.9889, 0.9971, which were pseudo-first order. Q_m, K_L, R^2 are 6.4382, 0.70533, 0.99923; 16.7364, 1.42059, 0.98816; 6.0078, 1.06973, 0.99889, respectively. The ΔH, ΔS, ΔS of -9.388, -0.024, -1.979; -27.182, -0.078, -3.592; -4.819, -0.017, 0.464 indicate the exothermic and spontaneous reaction. COD, TOC, pH, turbidity values have reached the threshold required by the government. The degradation products formed during the photodegradation-adsorption process were identified using LC-MS that the structure of the dye has been degraded to become simpler so that it is safely disposed of into the environment.

Keywords: Degradation product; dyes; TiO₂; chitosan; glass beads

1. INTRODUCTION

Synthetic dyes are widely used in the batik cloth dyeing process because of their very high absorption rate into textiles (Sarkar et al., 2020). The batik-making processes of dyeing, soaking, and washing, constantly release residual dyes, so these pollutants are most often found in the wastewater of the batik industry (Aoudjit et al., 2021). Most dyes have complex molecular structures because they contain several difficult benzene groups to degrade so that they can remain for a long time in water bodies. Waste released into the environment without treatment will undoubtedly cause a decrease in water quality and threaten aquatic ecosystems (Patehkhor et al., 2021).

Dyes in aquatic ecosystems block sunlight from penetrating the water surface, causing a reduction in rate. Increased organic matter and pH cause oxygen demand to increase and chemical species in water bodies to become harmful. Consuming water contaminated with dyes for a very long time will increase the potential for cancer, heart disease, gene mutations, allergies, tumors, and others (Srivastava et al., 2022). Therefore, an effort is needed to reduce dyes in the environment, one of which is using TiO₂-chitosan, which is immobilized on the surface of glass beads.

TiO₂ is the most widely used photocatalyst for degrading organic compounds due to its non-toxic, relatively cheap,

physically, and chemically stable, hydrophilic, and excellent photocatalytic activity under UV radiation (Djamila et al., 2020). Chitosan is a chitin deacetylation product that has high adsorption characteristics because it contains amino (NH_2) and hydroxyl (OH) functional groups and is non-toxic (Zhao et al., 2018). Using glass beads as a supporting material because they can be reused reduces the use of TiO_2-chitosan. The content of metal oxides, -NH_2, and -OH from TiO_2-chitosan immobilized on the surface of glass beads plays a role in reducing the concentration of dyes using a combination of photodegradation and adsorption so that the reaction runs more optimally (Rosdiana et al., 2023).

Thus far, the use of TiO_2-chitosan immobilized on the surface of glass beads for photodegradation-adsorption of dyes has only been carried out with a batch system without further identification of the degradation products (Aoudjit et al., 2021; Hoang et al., 2021; Tran et al., 2022). Batch photoreactors are more challenging to apply on a large scale than flow systems designed explicitly for photodegradation-adsorption processes, material usage, and low cost (Balarabe & Maity, 2022). Therefore, the flow system is used in this study to flow the feed and product continuously so that the contact between the solution and the material in the UV-C irradiated reactor is more even, and this system is also very efficient if applied on a large-scale, such as in the batik industry (Viriya, 2012). This study aims to determine the morphology and ability of TiO_2-chitosan immobilized on the surface of glass beads to reduce dye concentrations and identify kinetics, isotherms, thermodynamics, pH, COD, TOC, turbidity, and degradation products from a combination of photodegradation and adsorption using a flow system under UV-C radiation so that this material can be used for the treatment of batik industry wastewater containing dyes.

2. MATERIALS AND METHODS
Materials and Instruments

The materials used in this study are titanium (IV) oxide P-25 powder (718467 Sigma-Aldrich), chitosan (Bio Chitosan Indonesia), water (milli-Q), glass beads (BEAD-2000 Diversified Biotech), acetic acid (1000631000 Supelco Merck), sodium hydroxide (1064981000 Supelco Merck), methylene blue (556416 Sigma-Aldrich),

methyl orange (114510-25G Sigma-Aldrich), Rhodamine B, and batik industry wastewater (6°33'13.6 "S 106°49'20.2 "E).

The instruments used were UV-Vis Spectrophotometer (Cary 60 UV-Vis Spectrophotometer, Agilent Technology), Field Emission-Scanning Electron Microscopy - Energy Dispersive X-Ray (SEM-EDX) JIB-4610F and Ultra Performance Liquid Chromatograpy (UPLC) Xevo G2-S QTof.

Preparation of TiO_2-Chitosan Modified Glass Beads

Glass beads were prepared by soaking them in a 5% acetic acid solution for 12 hours at room temperature and then drying them in an oven. A total of 7.00 g of glass beads were sanded using SiC and then included in 25 mL of TiO_2-chitosan coating solution (2:1 (w/w)). Glass beads were coated using a casting technique by immersing them in the coating solution while heated at 80 °C for 4 hours. The dried glass beads were then placed in a 0.05 mol/L NaOH solution for 1 hour, washed with water to neutral pH, and dried at 55 °C for 1 hour. Glass beads were characterized using Field Emission-Scanning Electron Microscopy-Energy Dispersive X-Ray (FESEM-EDX) to identify the morphology and elements on the surface of the glass beads.

Photodegradation-Adsorption of Dyes by TiO_2-Chitosan Immobilized on The Surface of Glass Beads using a Flow System

TiO_2-chitosan that has been immobilized on the surface of glass beads is weighed as much as 27.00 g and put into a flow system reactor containing 60 mL of synthetic dyes (MB, RB, and MO) at 5.00 mg/L and batik industry wastewater for 135 minutes. The test results were analyzed quantitatively using a UV-Vis spectrophotometer at 665, 554, 464, 455, and 571 nm.

Kinetics, Isotherms, and Thermodynamics of Reactions

The reaction kinetics test was carried out by inserting TiO_2-chitosan immobilized on the surface of glass beads into a flow system reactor containing 5.00 mg/L synthetic dye for 120 minutes and then filtrating 1 mL at every 20-minute interval. Reaction isotherm tests were conducted by varying the initial concentration from 2, 4, 6, and 8 mg/L. The reaction thermodynamic test was determined by varying

the temperature during the reaction, namely 30 °C, 40 °C, 50 °C, and 60 °C.

Degradation Product Analysis

Initial and final samples of synthetic dyes and batik industry wastewater were measured for pH (SNI 6989.11:2019), COD (SNI 6989.73:2019), TOC, and turbidity (SNI 6989.25:2005). The filtrate from photodegradation-adsorption of synthetic dyes was analyzed using LC-MS. The LC system used an Ultra Performance Liquid Chromatography (UPLC) ACQUITY UPLC®H-Class System (waters, USA) equipped with a C18 ACQUITY UPLC® HSS column (1.8 m, 2.1 x 100 mm) (waters, USA) at 50°C. The mobile phases were the mixture of water and 5 mM ammonium formate (A), and acetonitrile with 0.05% formic acid (B) with a flow rate of 0.2 mL/min for 23 min. Samples were first filtered using a 0.2 m filter and injected as much as 5 l. The MS system was Xevo G2-S QTof (Waters, USA) with electrospray ionization (ES). Analysis was performed in the positive mode in the range of 50–1200 m/z, source temperature of 100 °C, desolvation temperature of 350 °C, cone gas flow of 0 L/hr, desolvation gas flow of 793 L/hr, collision energy of 4 volts (low energy), rampt collision energy of 25–60 volts (high energy).

3. RESULT AND DISCUSSION
TiO₂-Chitosan Immobilized on The Surface of Glass Beads

TiO₂-chitosan immobilized on the surface of glass beads is shown in **Figure 1(a)**. **Figure 1(b)** with a dark-colored surface is the surface of glass beads not coated by TiO₂-chitosan, while the light-colored surface is the surface of glass beads coated by TiO₂-chitosan (Vieira et al., 2019). **Figure 1(c)** shows that the surface of the glass beads has been perfectly coated by nanoparticle-sized TiO₂ photocatalysts (Amini-Badr & Behnajady, 2022). **Figure 1(d)** shows the EDX results of the surface already containing 5.2% Ti from TiO₂, 58.4% O and 25.5% C from chitosan, and 10.9% Si from using SiC. **Figure S1** shows the distribution of several elements, including Ti, O, C, and Si, which are homogeneous on the surface of glass beads that go through the coating process with TiO₂-chitosan.

(A)

(B)

(C)

(D)
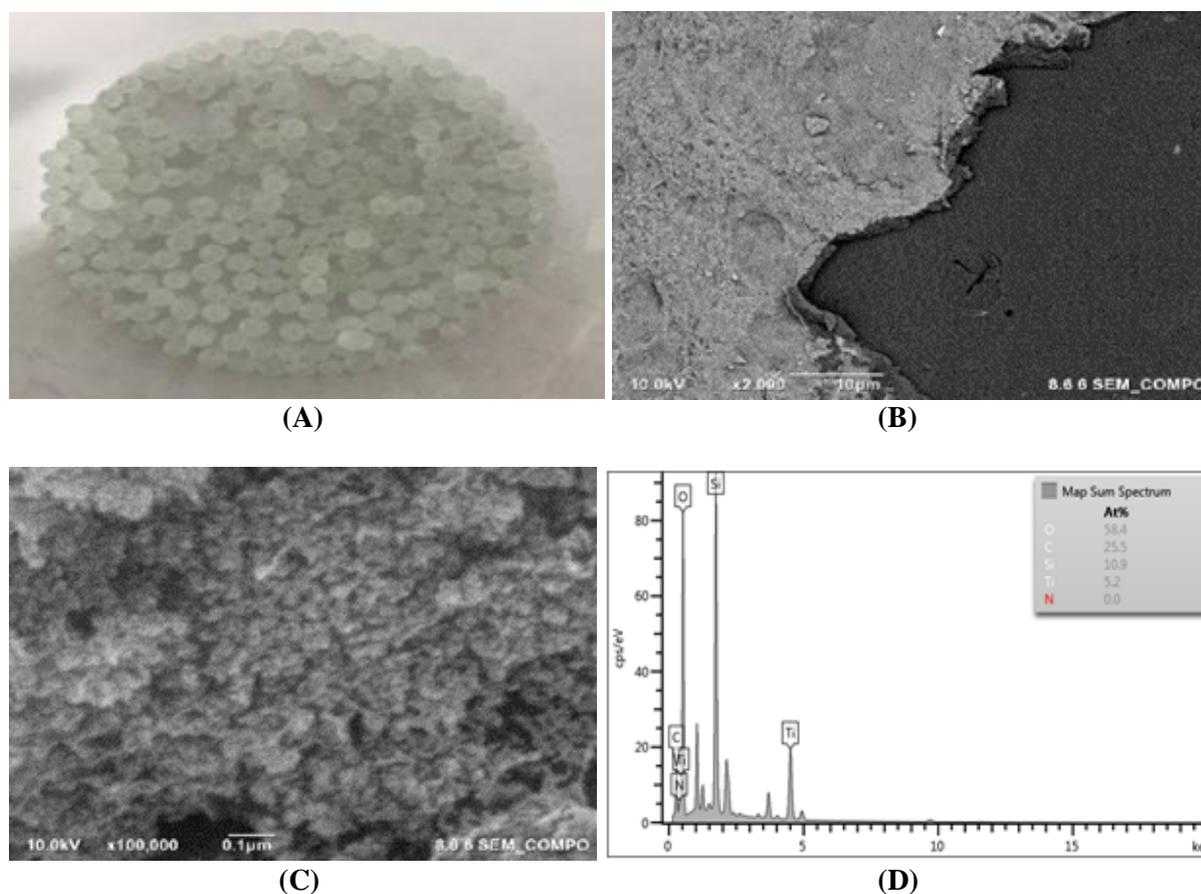
Figure 1. (a) TiO₂-chitosan immobilized on the surface of glass beads; (b) micrograms of the glass beads surface with magnification of 2,000x; (c) 100,000x; (d) EDX Results

Photodegradation-adsorption of dyes by TiO₂-Chitosan Immobilized on The Surface of Glass Beads using a Flow System

In this flow system, the pump and UV-C light source were kept on for 135 minutes to circulate and irradiate the solution. The efficiency of reducing the concentration of synthetic dyes (MB, MO, and RB) within 135 minutes was 98%, 99%, and 97%, respectively, as shown in **Figure 2**. The final concentrations of synthetic dyes after the photodegradation-adsorption process were 0.1 ppm, 0.05 ppm, and 0.15 ppm. The UV-Vis spectrum (**Figure 3**) shows that the decrease in MB and RB dyes is more dominant in photodegradation than MO dyes, which are more dominant in adsorption.

The efficiency of reducing the concentration of substances in wastes 1 and 2 within 135 minutes was 81% and 43%, respectively, as shown in **Figure 4**. The final concentration of synthetic dyes after the photodegradation-adsorption process was between 0.95 and 2.85 ppm. The higher photodegradation-adsorption efficiency of

waste 1 is due to the increased electrostatic attraction of negatively charged sulfonate groups with -NH₂ and -OH by chitosan, so the adsorption process is more dominant than photodegradation by TiO₂ (Hoang et al., 2021).
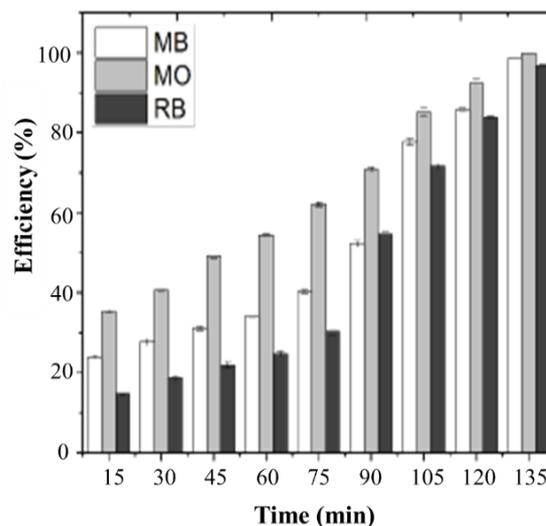
Figure 2. Synthetic dye concentration reduction efficiency.

(A)

(B)

(C)
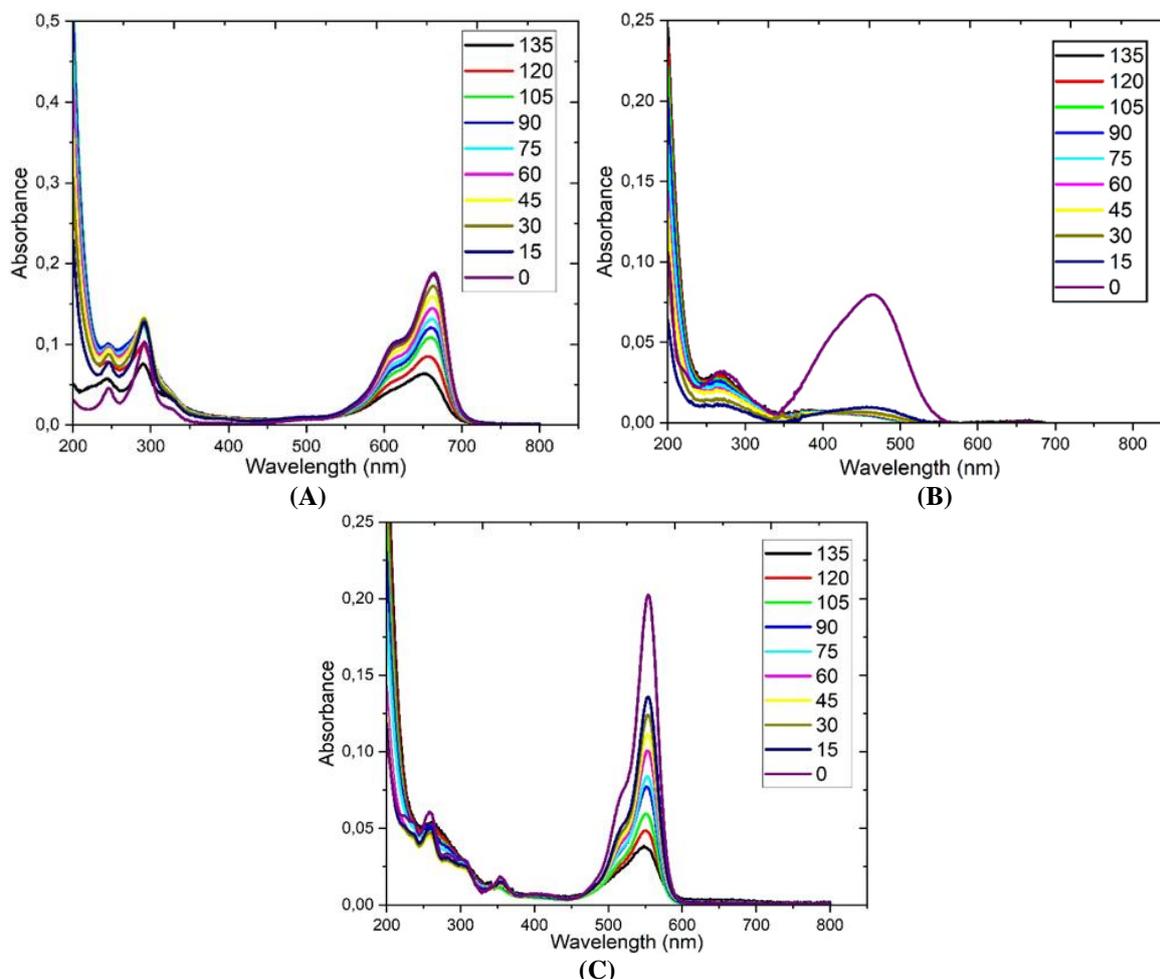
Figure 1. UV-Vis spectra of decreasing dye concentration (a) MB (b) MO (c) RB
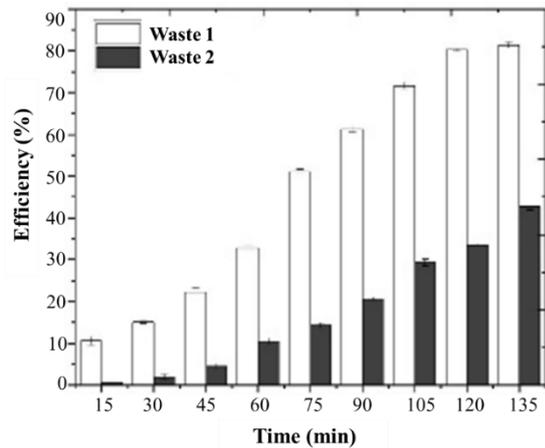
Figure 4. Efficiency of reducing dye concentration in batik industry wastewater

Isotherm, Kinetics, and Thermodynamics

The kinetics test determines the reaction order, while the reaction isotherm test shows the interaction between adsorbate molecules and the adsorbent surface by comparing R^2 values (Fathana et al., 2022). Thermodynamic tests are used to predict the spontaneity and nature of adsorbent interactions with dyes at equilibrium conditions using the influence of temperature. The calculation of the pseudo-first-order kinetics of synthetic dyes can be formulated in Equation 1:

$$ln[dye]_t = ln[dye]_0 + k\,t \quad \dots\dots\dots\dots(1)$$

The R^2 values were obtained by plotting time (x-axis) against $ln[dye]t$ (y-axis), as shown in **Figure 5(a)**. The calculation of the second-order kinetics of all synthetic dyes can be formulated in Equation 2:

$$\frac{1}{[dye]_t} = \frac{1}{[dye]_0} + k\,t \quad \dots\dots\dots\dots\dots\dots(2)$$

The R^2 value was obtained by plotting time (x-axis) against $1/[dye]t$ (y-axis), as shown in **Figure 5(b)**. Based on the linear regression equation and the correlation coefficient (R^2) in the reaction kinetics test shown in **Table 1**, the R^2 value closest to 1 is pseudo-first-order kinetics.
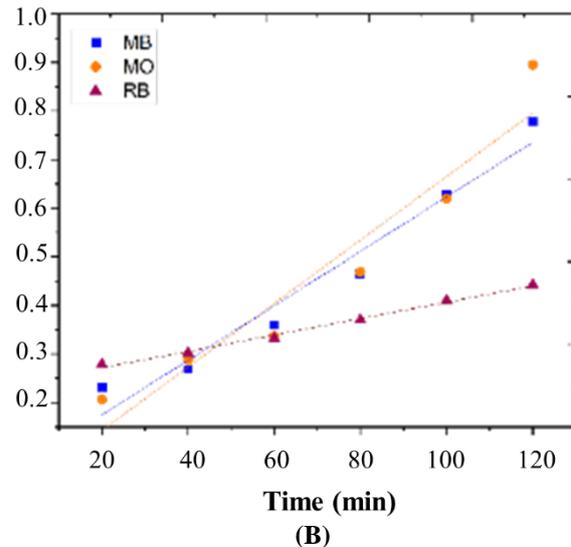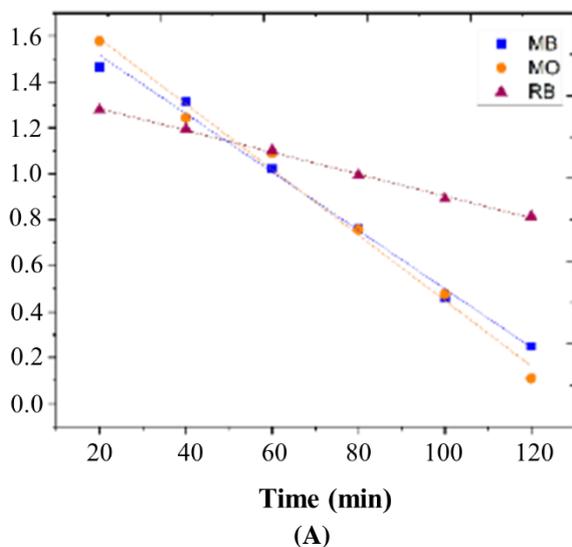
Figure 5. Model curves of (a) first pseudo-order kinetics (b) second pseudo-order kinetics

Table 1. Linear regression equation and correlation coefficient (R^2) of reaction kinetics test

	First pseudo-order		**Second pseudo-order**	
	Regression equation	**R^2**	**Regression equation**	**R^2**
MB	y= -0.01271x + 1.77024	0.99234	y= 0.00561x + 0.06246	0.95057
MO	y= -0.01424x + 1.87324	0.9889	y= 0.00653x + 0.01186	0.90322
RB	y= -0.00476x + 1.37976	0.9971	y= 0.00169x + 0.23791	0.99186

The photodegradation-adsorption reaction isotherm of synthetic dyes by TiO_2-chitosan immobilized on the surface of glass beads using a flow system is determined using two models, namely the Langmuir isotherm where the interaction is monolayer and the Freundlich isotherm where the interaction is a multilayer (Boughrara et al., 2022). The Langmuir isotherm is obtained by plotting the value of $1/Ce$ (x-axis) against the value of $1/Qe$ (y-axis) as shown in **Figure 6(a)**, the value of K_L, and qm is obtained using Equation 3. While the Freundlich isotherm is obtained by plotting the value of Log Ce (x-axis) against Log Qe (y-axis), as shown in **Figure 6(b)**, the values of K_F and n are obtained through Equation 4. The calculation results of each equation can be seen in **Table 2**.

The mechanism of the photodegradation-adsorption reaction of synthetic dyes using TiO_2-chitosan immobilized on the surface of glass beads using the flow system is the Langmuir isotherm, as evidenced by the value of R^2 closer to 1.

The photodegradation-adsorption process of synthetic dyes using TiO_2-chitosan immobilized on the surface of glass beads using a flow system was identified by calculating several thermodynamic parameters, namely enthalpy change (ΔH), entropy change (ΔS), and Gibbs free energy change (ΔG) (Sultana et al., 2022). The thermodynamic parameters were determined using the Van't Hoff equation (Equation 5) by plotting ln (Qe/Ce) (y-axis) and $1/T$ (x-axis) listed in **Figure 7**. The results of the test calculations on the thermodynamic parameters are shown in **Table 3**.

$$\frac{1}{qe} = \frac{1}{qm} + \frac{1}{Kl.qm}\frac{1}{Ce} \quad\ldots\ldots\ldots\ldots\ldots\ldots\ldots\ldots\ldots(3)$$

$$log\, Qe = log\, K_F + \frac{1}{n} log\, Ce \quad\ldots\ldots\ldots\ldots\ldots(4)$$

$$ln\, k = \frac{\Delta S}{R} - \frac{\Delta H}{RT} \quad\ldots\ldots\ldots\ldots\ldots\ldots\ldots\ldots\ldots\ldots\ldots(5)$$
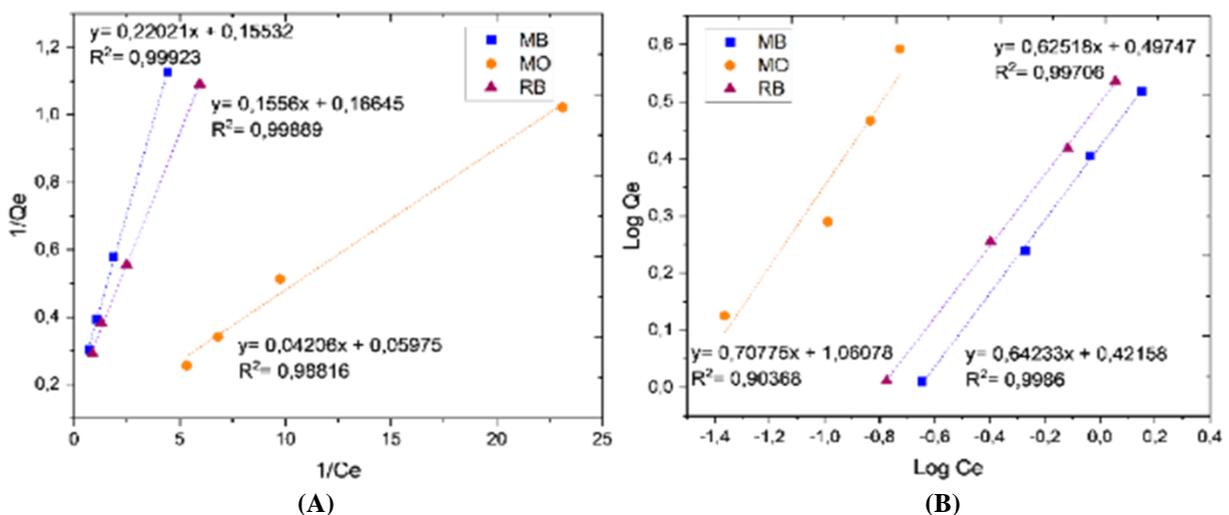
Figure 6. Linear regression curves of (a) Langmuir (b) Freundlich isotherm

Table 2. Langmuir and Freundlich isotherm test results

Dye	Langmuir			Freundlich		
	Qm	**K_L**	**R^2**	**K_F**	**n**	**R^2**
MB	6.43832	0.70533	0.99923	2.63985	1.55683	0.9986
MO	16.7364	1.42059	0.98816	11.5022	1.41293	0.90368
RB	6.00781	1.06973	0.99889	3.14391	1.59954	0.99706
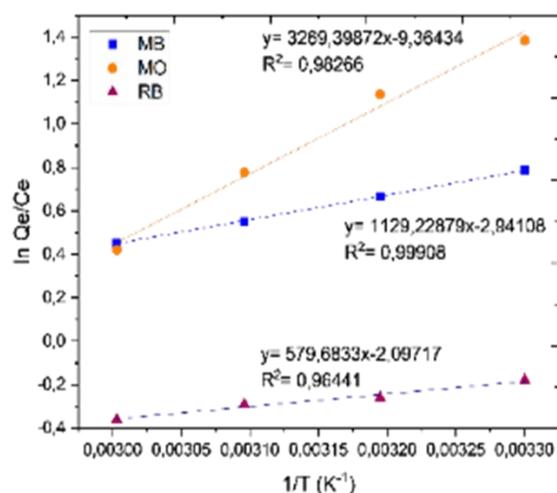
Figure 2. Linear regression curve of reaction thermodynamics

ΔH indicates the interaction between adsorbate molecules and the adsorbent surface (Bernal et al., 2020). A negative ΔH value indicates that the photodegradation-adsorption process of synthetic dyes by TiO₂-chitosan immobilized on the surface of glass beads is exothermic and physisorption (Abbasi & Ikram, 2022). Negative ΔS indicates that the dye molecules adsorbed to the surface of TiO₂-chitosan immobilized on the surface of glass beads have decreased irregularity. Negative ΔG indicates that the reaction takes place spontaneously. In contrast, positive ΔG indicates that photodegradation-adsorption of dyes using TiO₂-chitosan immobilized on the surface of glass beads is more challenging.

Environmental Parameter Test

In this study, pH, COD, TOC, and turbidity measurements were also tested to determine the effect of photodegradation-adsorption, as shown in **Table 4**. Based on the results of pH, COD, TOC, and turbidity measurements, the photodegradation-adsorption process of synthetic dyes and batik industry wastewater by TiO₂-chitosan immobilized on the surface of glass beads using a flow system can reduce these values to below the threshold set by the Regulation of the Minister of Environment of the Republic of Indonesia No. 5 of 2014 concerning Textile Wastewater Quality Standards.

Analysis of Synthetic Dye Degradation Products

The decrease in dye concentration and formation of new degradation products were identified using the LC system by observing the decrease and increase in height and peak area at specific retention times. **Figure 8(a)** shows a decrease in height with a peak area of MB at a retention time of 7.258 minutes, while at a retention time of 17.079 minutes, there is an increase in height with a peak area. **Figure 8(b)** shows a decrease in height with the peak area of MO at a retention time of 7.061 minutes, while at 16.326; 16.77; and 17.142 minutes, there was an increase in height with the peak area. **Figure 8(c)** shows a decrease in height with the peak area of RB at retention times of 9.802, 10.702, and 16.812 minutes. The degradation process is categorized as successful if the peak and peak area of the chromatogram has shown a decrease, which indicates a decrease in dye concentration, or an increase, which indicates the formation of other degradation products (Joshi et al., 2016; Prashantha et al., 2019; Rasheed et al., 2018).

Table 3. Test results on reaction thermodynamic parameters

Temperature (K)	MB			MO			RB		
	ΔH	ΔS	ΔG	ΔH	ΔS	ΔG	ΔH	ΔS	ΔG
303			-1.979			-3.592			0.464
313	-9.388	-0.024	-1.735	-27.182	-0.078	-2.813	-4.819	-0.017	0.638
323			-1.490			-2.035			0.812
333			-1.246			-1.256			0.987

ΔH= kJ/mol; ΔS= kJ/mol.K; ΔG= kJ/mol

Table 4. pH, COD, TOC, and turbidity of wastewater

	MB		MO		RB		Waste 1		Waste 2	
Time (minutes)	0	120	0	120	0	120	0	120	0	120
pH	6.59	7.13	6.54	7.19	6.56	7.18	8.40	8.22	8.24	8.12
COD	45.9	22	77.1	11	77.08	7.34	1083	407	2317	673
TOC	0.06	0.05	0.05	0.02	0.05	0.04	0.09	0.06	0.17	0.06
Turbidity	30.6	5.83	18.2	0.13	20.2	19	583	102	300	62.9

COD (mg/L); TOC (%v/v); turbidity (NTU)

(A)

(B)

(C)
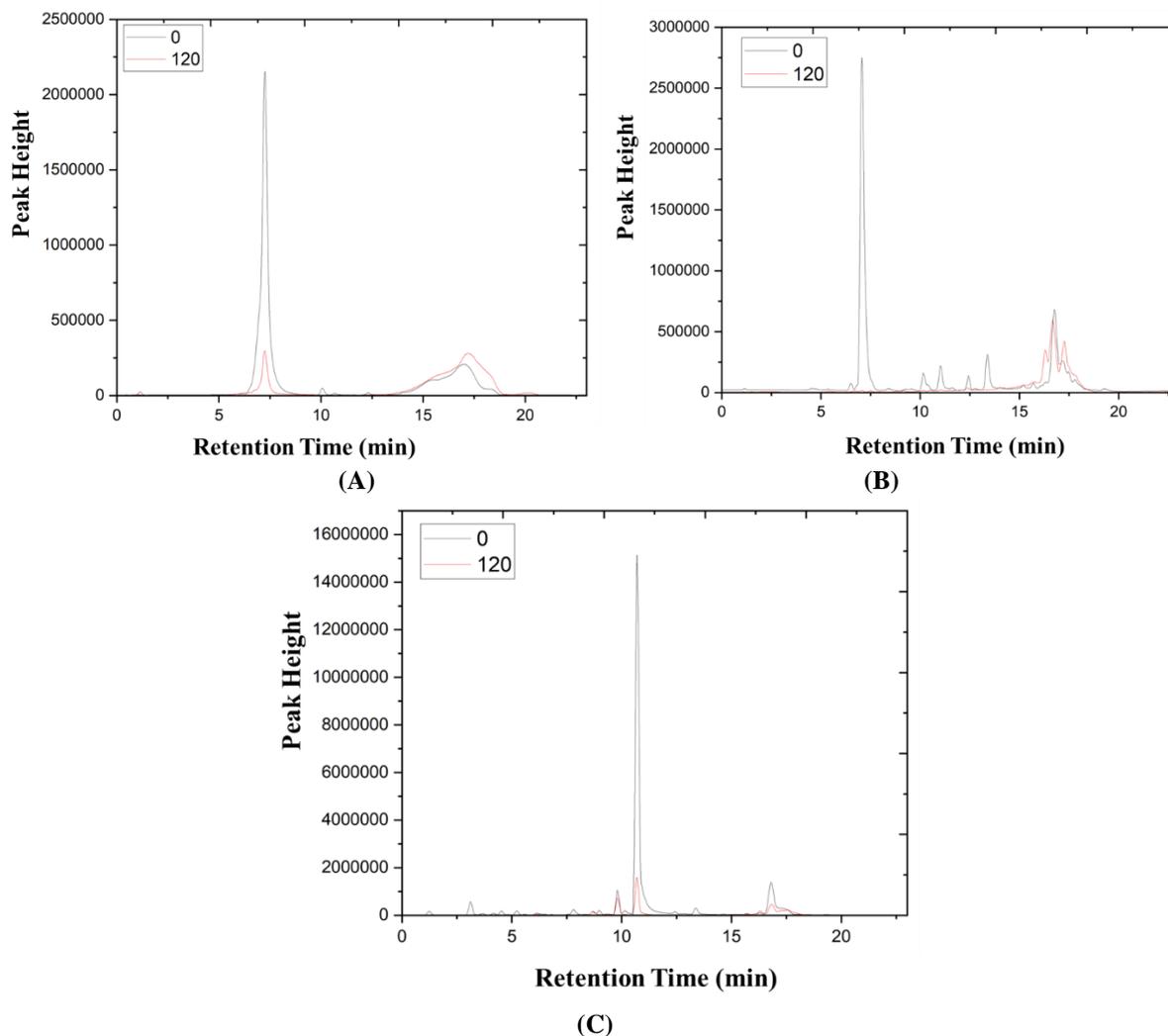
Figure 8. LC chromatogram of (a) MB (b) MO (c) RB

The degradation products during the photodegradation-adsorption process were further identified using MS by observing the decrease and increase in spectral height at certain retention times to determine the molecular formula and structure. **Figure 9(a)** shows the spectra with a single peak with high intensity at m/z 284, identified as an MB molecule, as described in **Table 5**. After 120 minutes, the spectral intensity of the MB molecule decreased and formed spectra with a smaller m/z, indicating the beginning of the breakdown of the main structure of MB shown in **Figure 9(b)**.
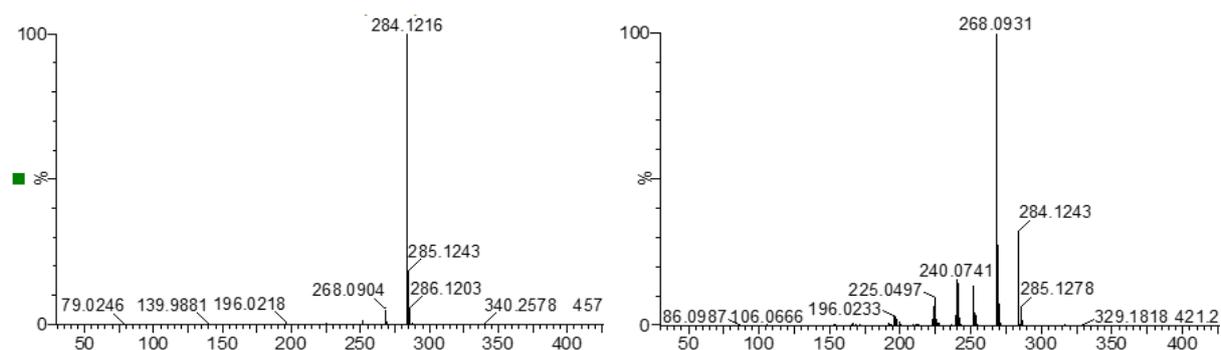
Figure 9. MS spectrum of photodegradation-adsorption of MB dye at (a) 0 min (b) 120 min

Table 5: Formula and molecular structure of final product of MB degradation

m/z	Molecular Formula	Structure	m/z	Molecular Formula	Structure
284	$C_{16}H_{18}N_3S$		240	$C_{13}H_{10}N_3S$	
268	$C_{15}H_{14}N_3S$				
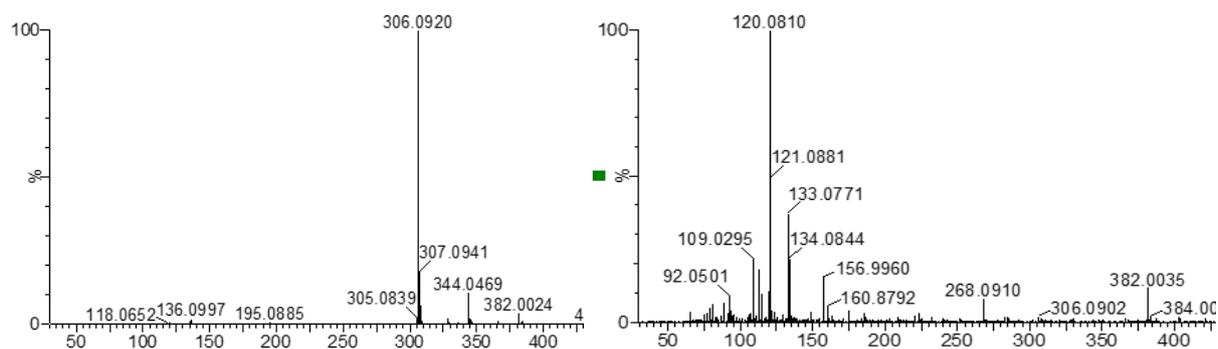
Figure 10. MS spectrum of photodegradation-adsorption of MO dye at (a) 0 min (b) 120 min

Further identification results explain that m/z 268, 240, and 225 are still MB molecules with structures that have lost some side groups. The change in the peak at m/z 284 to a peak at m/z 268 indicates a methane (CH_4) removal reaction from the MB molecule. The peak at m/z 240 results from removing one of the dimethylamine groups from MB. The photodegradation process has not obtained final products in the form of CO_2, H_2O, and other organic materials that are more stable and environmentally friendly; it is expected that if the photodegradation-adsorption process is carried out longer, more simple final products will be formed (Nguyen et al., 2019).

Figure 10(a) shows a single peak with high intensity at m/z = 306.0920, identified as an MO molecule, as listed in **Table 6**. After 120 min, the MO molecule was no longer visible,

and several new peaks with varying heights were formed, as shown in **Figure 10(b)**. Some new peaks identified are at m/z 92, 109, 120, 121, 133, 134, and 156, indicating that new degradation products have been formed (Ren et al., 2022).

The peak change from m/z 306, which has lost Na^+ ions due to dissolution with water, to a reasonably high peak at m/z 120 and 121 indicates the removal of amino groups (NH_2) from the MO molecule (Sun et al., 2020). The MO molecule can also degrade into a peak at m/z 157, benzene sulfonic acid (Kgatle et al., 2021). The peak at m/z 109 indicates the formation of 4-aminophenol derived from the presence of two free radicals (HO) at each N and O of 4-(hydroxyamino) phenol (Riaz et al., 2015).

Table 1. Formula and molecular structure of final product of MO degradation

m/z	Molecular Formula	Structure	m/z	Molecular Formula	Structure
306	$C_{13}H_{12}N_3O_4S$		157	$C_6H_5O_3S$	
121	$C_8H_{11}N$		109	C_6H_7NO	
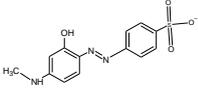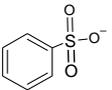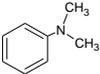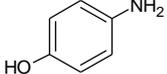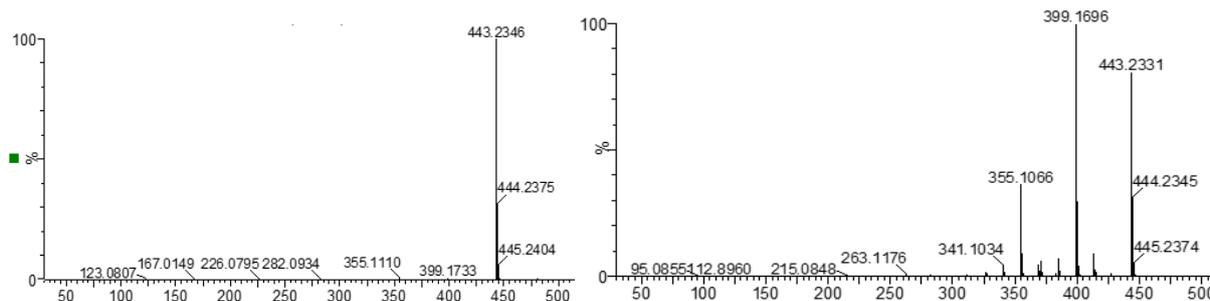
Figure 11. MS spectra of RB dye removal at (a) 0 min (b) 120 min.

Table 7. Formula and molecular structure of final product of RB degradation

m/z	Molecular Formula	Structure	m/z	Molecular Formula Structure	
443	$C_{28}H_{31}N_2O_3$		355	$C_{19}H_{19}N_2O_5$	
399	$C_{27}H_{31}N_2O$				
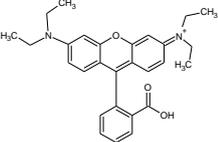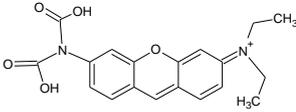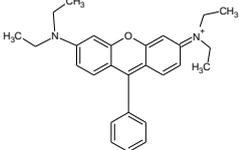
Figure 11(a) shows a single peak with high intensity at m/z 443.2348 that was identified as an RB molecule. After 120 minutes, the RB molecule still appears but with a lower intensity, and a new peak is formed, as shown in **Figure 11(b)**, which can be attributed to the formation of other intermediates that are the result of RB degradation (Eddy et al., 2022). The formula and molecular structure of RB shown in **Table 7** at 0 minutes are those of RB that have lost Cl-ions due to dissolution with water. The peak change from m/z 443 to m/z 399 resulted from the loss of carboxyl groups from the RB parent structure (Eddy et al., 2022).

4. CONCLUSIONS

Based on the FE-SEM EDX results, TiO$_2$-chitosan has coated homogeneously on the surface of the glass beads. Using a flow system can increase the effectiveness of reducing the concentration of synthetic dyes and batik industry wastewater. Based on aspects of kinetics, isotherms, and thermodynamics, photodegradation-adsorption of synthetic dyes by TiO$_2$-chitosan immobilized on the surface of glass beads using a flow system follows pseudo-first-order kinetics with Langmuir isotherms and occurs exothermically and spontaneously. The reduction of pH, COD, TOC, and turbidity

values gave satisfactory results, reaching 80%, thus meeting the threshold required by the government. Identification of photodegradation structures and products by LC chromatograms and MS spectra showed that the three synthetic dyes had been degraded into more superficial structures likely to be more easily decomposed by organisms.

ACKNOWLEDGMENTS

REFERENCES

Abbasi, A., Ikram, S. (2022). Fabrication of a novel green bio-composite for sequestration of Victoria Blue from aquatic medium: Isotherm, Kinetics, and Thermodynamic investigations. *Chemical Physics Letters*, *800*(April), 139665. https://doi.org/10.1016/j.cplett.2022.139665

Amini-Badr, A., Behnajady, M. A. (2022). Photocatalytic removal of cefazolin in a photoreactor packed with TiO₂-P25 nanoparticles supported on glass beads: an artificial neural network modeling. *International Journal of Environmental Analytical Chemistry*, *00*(00), 1–19. https://doi.org/10.1080/03067319.2022.2130060

Aoudjit, L., Zioui, D., Touahra, F., Mahidine, S., Bachari, K. (2021). Photocatalytic degradation of tartrazine dyes using TiO₂–chitosan beads under sun light irradiation. *Russian Journal of Physical Chemistry A*, *95*(5), 1069–1076. https://doi.org/10.1134/S0036024421050034

Balarabe, B. Y., Maity, P. (2022). Visible light-driven complete photocatalytic oxidation of organic dye by plasmonic Au-TiO₂ nanocatalyst under batch and continuous flow condition. *Colloids and Surfaces A: Physicochemical and Engineering Aspects*, *655*(August), 130247. https://doi.org/10.1016/j.colsurfa.2022.130247

Bernal, V., Giraldo, L., Moreno-Piraján, J. C. (2020). Insight into adsorbate–adsorbent interactions between aromatic pharmaceutical compounds and activated carbon: equilibrium isotherms and thermodynamic analysis. *Adsorption*, *26*(2), 153–163. https://doi.org/10.1007/s10450-019-00057-x

Bläker, C., Pasel, C., Luckas, M., Dreisbach, F., Bathen, D. (2017). Investigation of load-dependent heat of adsorption of alkanes and alkenes on zeolites and activated carbon. *Microporous and Mesoporous Materials*, *241*, 1–10. https://doi.org/10.1016/j.micromeso.2016.12.037

Boughrara, L., Zaoui, F., Guezzoul, M., Sebba, F. Z., Bounaceur, B., Kada, S. O. (2022). New alginic acid derivatives ester for methylene blue dye adsorption: kinetic, isotherm, thermodynamic, and mechanism study. *International Journal of Biological Macromolecules*, *205*(February), 651–663. https://doi.org/10.1016/j.ijbiomac.2022.02.087

Djamila, Z., Hugo S., Lamine A., Pedro M. M., Senentxu, L. M. (2020). Polymer-based membranes for oily wastewater remediation. *Polymers*, *12*(42). https://doi.org/10.3390/polym12010042

Eddy, D. R., Nursyamsiah, D., Permana, M. D., Solihudin, Noviyanti, A. R., Rahayu, I. (2022). Green production of zero-valent iron (ZVI) using tea-leaf extracts for fenton degradation of mixed rhodamine b and methyl orange dyes. *Materials*, *15*(1). https://doi.org/10.3390/ma15010332

Fathana, H., Rahmi, R. Lubis, S., Adlim, M., Muktaridha, O., Ikhramullah, M. (2022). Fabrication and investigation of new TiO₂/amino acids modified chitosan for methylene blue removal via adsorption and photodegradation. *Research square*. https://doi.org/10.21203/rs.3.rs-1777346/v1

Hoang, N. T. T., Tran, A. T. K., Hoang, M. H., Nguyen, T. T. H., Bui, X. T. (2021). Synergistic effect of TiO₂ /chitosan/glycerol photocatalyst on color and COD removal from a dyeing and textile secondary effluent. *Environmental Technology and Innovation*, *21*, 101255. https://doi.org/10.1016/j.eti.2020.101255

Joshi, S., Ippolito, S. J., Sunkara, M. V. (2016). Convenient architectures of Cu₂O/SnO₂ type II p-n heterojunctions and their application in visible light catalytic degradation of rhodamine B. *RSC Advances*, *6*(49), 43672–43684. https://doi.org/10.1039/c6ra07150c

Kgatle, M., Sikhwivhilu, K., Ndlovu, G., Moloto, N. (2021). Degradation kinetics of methyl orange dye in water using. *Catalysts*, *11*, 428. https://doi.org/10.3390/catal11040428

Nguyen, T. B., Doong, R. an, Huang, C. P., Chen, C. W., Dong, C. Di. (2019). Activation of persulfate by CoO nanoparticles loaded on 3D mesoporous carbon nitride (CoO@meso-CN) for the degradation of methylene blue (MB). *Science of the Total Environment*, *675*, 531–541. https://doi.org/10.1016/j.scitotenv.2019.04.230

Patehkhor, H. A., Fattahi, M., Khosravi-Nikou, M. (2021). Synthesis and characterization of ternary chitosan–TiO_2–ZnO over graphene for photocatalytic degradation of tetracycline from pharmaceutical wastewater. *Scientific Reports*, *11*(1), 1–17. https://doi.org/10.1038/s41598-021-03492-5

Prashantha Kumar, T. K. M., Ashok Kumar, S. K. (2019). Visible-light-induced degradation of rhodamine B by nanosized Ag_2S-ZnS loaded on cellulose. *Photochemical and Photobiological Sciences*, *18*(1), 148–154. https://doi.org/10.1039/c8pp00330k

Rasheed, T., Bilal, M., Iqbal, H. M. N., Shah, S. Z. H., Hu, H., Zhang, X., Zhou, Y. (2018). TiO_2/UV-assisted rhodamine B degradation: putative pathway and identification of intermediates by UPLC/MS. *Environmental Technology (United Kingdom)*, *39*(12), 1533–1543. https://doi.org/10.1080/09593330.2017.1332109

Ren, Z., Wang, Z., Lv, L., Ma, P., Zhang, G., Li, Y., Qin, Y., Wang, P., Liu, X., Gao, W. (2022). Fe–N complex biochar as a superior partner of sodium sulfide for methyl orange decolorization by combination of adsorption and reduction. *Journal of Environmental Management*, *316*(April), 115213. https://doi.org/10.1016/j.jenvman.2022.115213

Riaz, U., Ashraf, S. M., Farooq, M. (2015). Effect of pH on the microwave-assisted degradation of methyl orange using poly(1-naphthylamine) nanotubes in the absence of UV–visible radiation. *Colloid and Polymer Science*, *293*(4), 1035–1042. https://doi.org/10.1007/s00396-014-3485-4

Rosdiana, E. A., Basid, N., Prasetya, A., Gunawan, G. (2023). Synthesis and characterization of

TiO_2-chitosan beads and its application as a degradation agent of methylene blue. *Trends in Sciences*, 20(9). DOI:10.48048/tis.2023.6670

Sarkar, S., Banerjee, A., Chakraborty, N., Soren, K., Chakraborty, P., Bandopadhyay, R. (2020). Structural-functional analyses of textile dye degrading azoreductase, laccase and peroxidase: A comparative in silico study. *Electronic Journal of Biotechnology*, *43*, 48–54. https://doi.org/10.1016/j.ejbt.2019.12.004

Srivastava, V., Choubey, a. K. (2022). Novel PVA/chitosan composite membrane modified using bio fabricated α-MnO_2 nanoparticles for photocatalytic degradation of cationic dyes. *Environmental Science and Pollution Research, 30*: 35838–35852. https://doi.org/10.21203/rs.3.rs-1393311/v1

Sultana, T., Dey, S. C., Molla, M. A. I., Hossain, M. R., Rahman, M. M., Quddus, M. S., Moniruzzaman, M., Shamsuddin, S. M., Sarker, M. (2021). Facile synthesis of TiO_2/Chitosan nanohybrid for adsorption-assisted rapid photodegradation of an azo dye in water. *Reaction Kinetics, Mechanisms and Catalysis*, *133*(2), 1121–1139. https://doi.org/10.1007/s11144-021-02009-5

Sun, X., Xu, D., Dai, P., Liu, X., Tan, F., Guo, Q. (2020). Efficient degradation of methyl orange in water via both radical and non-radical pathways using Fe-Co bimetal-doped MCM-41 as peroxymonosulfate activator. *Chemical Engineering Journal*, *402*(May), 125881. https://doi.org/10.1016/j.cej.2020.125881

Tran, A. T. K., Hoang, N. T. T., Nguyen, T. T. H. (2022). Combination of photocatalytic degradation and adsorption in dye removal by TiO2-chitosan-glycerol beads under natural sunlight. *IOP Conference Series: Earth and Environmental Science*, *964*(1). https://doi.org/10.1088/1755-1315/964/1/012028

Vieira, M. L. G., Pinheiro, C. P., Silva, K. A., Lutke, S. F., Cadaval, T. R. S. A., Dotto, G., Pinto, L. A. de A. (2019). Chitosan and cyanoguanidine-crosslinked chitosan coated glass beads and its application in fixed bed adsorption. *Chemical Engineering Communications*, *206*(11), 1485–1497. https://doi.org/10.1080/00986445.2019.1581618

Viriya, K. (2012). *Uji Kinerja Fotoreaktor Silinder Berputar Skala Pilot Untuk Pengolahan Limbah Fenol Dengan Menggunakan Katalis* *TiO$_2$/ZAL.* Fakultas teknik program studi teknik kimia Universitas Indonesia.